WAVELET BASED EVENT DETECTION IN PACEMAKERS

M. Åström, S. Olmos, L. Sörnmo
Department of Electroscience, Lund University, Lund, Sweden

Abstract— **This paper presents a detection algorithm for pacemakers which is based on a signal model including a linear combination of descriptive functions. The functions are defined as different time scales of the two fundamental waveforms in the electrogram. An efficient detector structure is provided by the use of a dyadic wavelet transform with integer filter coefficients, followed by a generalized likelihood ratio test. The results show that reliable detection can be obtained for moderate to high noise levels for some common noise sources.**

Keywords— **Detection, electrogram, generalized likelihood ratio test, pacemaker, sensing, wavelet**

I. Introduction

During the last four decades, an impressive development in pacemaker technology has taken place. Features such as hermetical sealing, programmability, telemetry, circuit redundancy and rate responsive pacing have been added in order to increase functionality and reliability [1]. However, the basic event detection (or sensing) algorithm remains more or less unchanged, still based on bandpass filtering followed by an amplitude threshold. So far, IC miniaturization has made limited impact in this field.

During the last twenty years, a large amount of surface electrocardiogram (ECG) QRS detection algorithms have been presented. However, event detection using the electrogram (EGM) introduces new demands disqualifying most ECG QRS detection algorithms. In a pacemaker the decision must be made in real time with a delay of no more than approximately 40 ms in order to pace safely. Furthermore, pacemaker implementation introduces power constraints which, in general make ECG QRS detection algorithms too complex to be considered.

The need for better event (R wave[1]) detectors in pacemakers is ever increasing. An external noise source can essentially interfere with a pacemaker in one or several ways [2]. During the last decades, an increasing amount of electrical equipment has been introduced to the general public which may be potential threats to pacemaker functionality. This has been the topic of several studies in recent years, where specific types of interference are investigated e.g., from cellular phones, magnetic resonance imaging (MRI) and electronic article surveillance (EAS) systems. The overall conclusions from these studies were that for cellular phones no increased risk of pacemaker malfunction exists [3]. For MRI, an increased risk and even deaths may be related to malpractice of pacemaker patients [4]. Also in EAS systems the risk of malfunction increases. However, these devices all affect pacemakers in varying degrees due to the widely spread surveillance techniques, making individual investigations necessary [5], [6]. Moreover, internal muscle noise interferes with pacemakers [7].

This paper includes a short description of the material used for evaluation. Next, the detection algorithm is presented including the signal model with the resulting detector structure and a complexity analysis of the algorithm. Evaluation results of the algorithm are presented for some common interference signals. Finally, the detector structure is briefly discussed.

This project was supported by St. Jude Medical, Stockholm, Sweden.

[1]The waveform corresponding to ventricular depolarization is here, as in many other papers, referred to as the R wave although this terminology is defined for the surface ECG.

II. Materials

In order to evaluate detection performance, an EGM database with 50 recordings and an interference database were combined.

A. EGM signals

The database contains EGMs from patients in different German hospital clinics, coordinated at the Justus-Liebig Universität in Gießen, Germany. All EGM recordings were made from pacemaker electrodes during e.g., pacemaker implant or replacement, under controlled and relatively noisefree conditions. In this study, 50 ventricular recordings sampled at 1 kHz were used for evaluation. The database includes subjects with no heart disease at the recording opportunity, patients with AV blocks and sick sinus syndrome.

In order to be able to use the database for evaluation of event detection algorithms, the beats were annotated. After annotation, all files were visually inspected, verified and modified if necessary.

B. Interference

An interference database was used in order to quantify the performance in common noisy situations. The database, provided by St. Jude Medical, Stockholm, Sweden, contains the following noise sources, cf. Fig. 1:

- *Electronic article surveillance* systems, where two models operating within the same frequency band as the R wave have been tested. The two models are the System 2500 from Esselte Meto AB, Solna, Sweden and the Ultramax from Sensormatic Inc, Boca Raton, FL, USA.
- *Household appliances,* which affect through electric and magnetic interference usually with a fundamental tone of 50 – 60 Hz, approximately in the same frequency range as the R wave [8]. An AC powered drill and an electric hand mixer were used for this group.
- *Muscular activity,* which is a wideband noise source and, to a certain degree, spans the same frequency band as myocardial signals.

Report Documentation Page

Report Date	Report Type	Dates Covered (from... to)
25 Oct 2001	N/A	-

Title and Subtitle Wavelet Based Event Detection in Pacemakers	**Contract Number**
	Grant Number
	Program Element Number
Author(s)	**Project Number**
	Task Number
	Work Unit Number
Performing Organization Name(s) and Address(es) Department of Electroscience Lund University Lund Sweden	**Performing Organization Report Number**
Sponsoring/Monitoring Agency Name(s) and Address(es) US Army Research, Development & Standardization Group (UK) PSC 802 Box 15 FPO AE 09499-1500	**Sponsor/Monitor's Acronym(s)**
	Sponsor/Monitor's Report Number(s)

Distribution/Availability Statement
Approved for public release, distribution unlimited

Supplementary Notes
Papers from 23rd Annual International Conference of the IEEE Engineering in Medicine and Biology Society, October 25-28, 2001, held in Istanbul, Turkey. See also ADM001351 for entire conference on cd-rom. , The original document contains color images.

Abstract

Subject Terms

Report Classification unclassified	**Classification of this page** unclassified
Classification of Abstract unclassified	**Limitation of Abstract** UU

Number of Pages
4

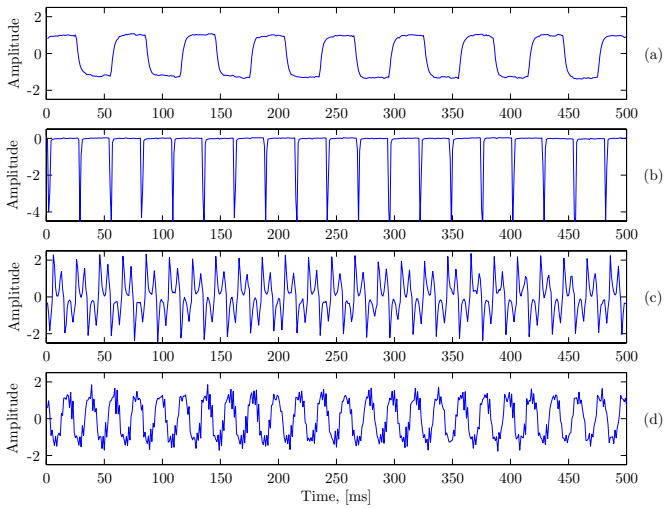

Fig. 1. External interference signals. The signals are originating from Esselte System 2500 EAS system in (a), Sensormatic's Ultramax EAS system in (b), a 500 W power drill in (c) and an electric hand mixer in (d).

C. Signal-to-noise ratio definition

A signal-to-noise ratio was defined in order to investigate noise levels for satisfactory operation. The peak-to-peak QRS amplitude was used as signal measure and for the noise its standard deviation. An example of a noisy EGM with myo-muscular noise (20 dB SNR) is shown in Fig. 2.

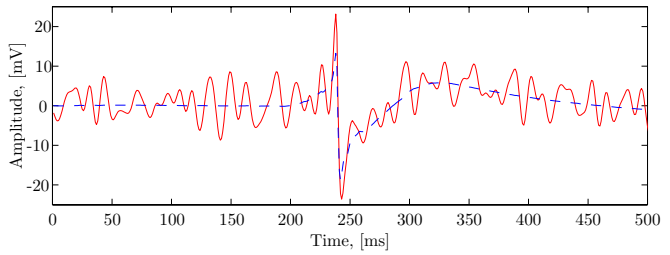

Fig. 2. Example of an EGM segment with a 20 dB SNR from myo-muscular noise.

III. Event detection

Most present ECG QRS detectors are based on the same basic structure. A linear filter, followed by some nonlinear transformation which conditions the signal prior to the decision rule. This is also the case for present EGM R wave detectors for implantable devices which generally are very simple implementations including a bandpass filter and an amplitude threshold.

A. Signal model

The EGM R wave morphology is generally more heterogeneous than the ECG QRS. In order to model the EGM R wave, the model should comprise a wide range of morphologies, as modelled by a small set of functions. In this paper, the assumption is that the R wave waveform is composed of a linear combination of representative functions,

$$\mathbf{H} = [\,\mathbf{h}_1 \;\ldots\; \mathbf{h}_p\,] \tag{1}$$

with $\mathbf{h}_j = [\,h_j(0) \;\ldots\; h_j(N-1)\,]^T$. The only restriction on $\mathbf{H}$ is that it must be full rank. The observed signal, $\mathbf{x} = [\,x(0) \;\ldots\; x(N-1)\,]^T$, is modelled as

$$\mathbf{x} = \mathbf{H}\boldsymbol{\theta} + \mathbf{w} \tag{2}$$

where $\boldsymbol{\theta}$ denotes the coefficient vector for the different waveforms and $\mathbf{w}$ is white Gaussian noise, $w(n) \in \mathcal{N}(0, \sigma_w^2)$.

Detection problems are commonly formulated in terms of hypothesis testing, choosing the more likely one. In this case the problem can be formulated as $\boldsymbol{\theta}$ is either zero, implying that no R wave is present, $\mathcal{H}_0$, or nonzero, implying that an R wave is present, $\mathcal{H}_1$,

$$\begin{aligned} \mathcal{H}_0 &: \quad \boldsymbol{\theta} = \mathbf{0} \\ \mathcal{H}_1 &: \quad \boldsymbol{\theta} \neq \mathbf{0} \end{aligned} \tag{3}$$

For the general case, of course, knowledge of $\boldsymbol{\theta}$ is not available, and therefore an estimate of $\boldsymbol{\theta}$ is required before hypothesis testing.

B. Signal representation

An important task in designing a robust detector is to determine an appropriate model of $\mathbf{H}$. It should be chosen such that it resembles the basic set of morphologies of the EGM. The optimal representation of an ensemble of signals is given by the Karhunen-Loève (KL) transform. Thus, the columns of $\mathbf{H}$ are constituted by the KL basis functions. However, a couple of aspects makes KL basis functions less attractive in a low complexity implementation. For example, it is desirable to calculate the estimate $\hat{\boldsymbol{\theta}}$ recursively which is not possible with the KL basis functions. It is also desirable to use small integer-based basis functions in order to calculate the coefficients whereas the KL basis functions are represented in floating point, implying large word lengths.

Instead of using KL basis functions, the starting point in modelling $\mathbf{H}$ has been to take advantage of *a priori* morphologic information of the R wave suggesting that it is composed of *symmetric* and *antisymmetric* waveforms [8]. One transform which may be implemented efficiently is the dyadic wavelet transform. By choosing proper filters, a symmetric and an antisymmetric filter bank are obtained. A filter, $f(n)$, is combined with either $g_s(n)$ or $g_a(n)$ (where subindices s and a denotes symmetric and antisymmetric, respectively) according to,

$$\begin{aligned} h_{1,\{s,a\}}(n) &= g_{\{s,a\}}(n) \\ h_{2,\{s,a\}}(n) &= f(n) * g_{\{s,a\}}(2n) \\ h_{3,\{s,a\}}(n) &= f(n) * f(2n) * g_{\{s,a\}}(4n) \\ &\vdots \\ h_{q,\{s,a\}}(n) &= f(n) * \ldots * f(2^{q-2}n) * g_{\{s,a\}}(2^{q-1}n) \end{aligned} \tag{4}$$

In (4), $f(n)$ was chosen as a third order spline function,

$$f(n) = [\ 1 \quad 3 \quad 3 \quad 1\ ] \tag{5}$$

For the antisymmetric filter bank, the filter, $g_a(n)$ was selected as the first order difference,

$$g_a(n) = [\ -1 \quad 1\ ] \tag{6}$$

The corresponding symmetric filter bank is given by $g_s(n)$ which was chosen as,

$$g_s(n) = g_a(n) * g_a(n) = [\ 1 \quad -2 \quad 1\ ] \tag{7}$$

It is now possible to present an expression for $\mathbf{H}$. In this paper, scales 2 – 4 in (4) have been used since they reflect the R wave well and introduce acceptable delays in the algorithm, resulting in,

$$\mathbf{H} = \left[\ \tilde{\mathbf{h}}_{2,b}\ \tilde{\mathbf{h}}_{3,b}\ \tilde{\mathbf{h}}_{4,b}\ \tilde{\mathbf{h}}_{2,m}\ \tilde{\mathbf{h}}_{3,m}\ \tilde{\mathbf{h}}_{4,m}\ \right] \tag{8}$$

where $\tilde{\mathbf{h}}_{j,\{s,a\}} = \left[\ h_{j,\{s,a\}}(N-1)\ \ldots\ h_{j,\{s,a\}}(0)\ \right]^T$. The reversed order is introduced in order to be consistent with the model assumed in (2).

Calculation of $\mathbf{H}$ does not require an efficient implementation since this is done only once and has no real time constraints. However, an efficient, recursive implementation of calculating the filter outputs, $\mathbf{H}^T\mathbf{x}$, from the two filter banks in (4) is convenient. This operation is known as Mallat's algorithm [9]. By using Mallat's algorithm it is possible to calculate both the symmetric and the antisymmetric filter output from each scale by using $f(n)$ once and $g_a(n)$ twice. By applying the *"algorithme a trous"*, downsampling of the signal from one scale to the next may be omitted.

C. GLRT detection

In order to decide on $\mathcal{H}_0$ or $\mathcal{H}_1$ in (3), a generalized likelihood ratio test (GLRT) is used [10]. The test statistic $T(\mathbf{x})$ is compared to a threshold, γ, in order to decide between $\mathcal{H}_0$ and $\mathcal{H}_1$,

$$T(\mathbf{x}) = \frac{p\left(\mathbf{x}; \hat{\boldsymbol{\theta}}_1, \mathcal{H}_1\right)}{p\left(\mathbf{x}; \hat{\boldsymbol{\theta}}_0, \mathcal{H}_0\right)} \begin{matrix} > \\ < \end{matrix} \gamma \quad \begin{matrix} \mathcal{H}_1 \\ \mathcal{H}_0 \end{matrix} \tag{9}$$

The test is a comparison of the probability of $\mathbf{x}$ given $\hat{\boldsymbol{\theta}}_1$ which is the maximum likelihood estimate (MLE) of $\boldsymbol{\theta}_1$ assuming $\mathcal{H}_1$ relative to the probability of $\mathbf{x}$ given $\hat{\boldsymbol{\theta}}_0$ which is the MLE of $\boldsymbol{\theta}_0$ assuming $\mathcal{H}_0$.

When $\mathbf{w}$ is assumed to be stationary and characterized by a Gaussian probability density function, then (9) may be reformulated to,

$$T(\mathbf{x}) = \frac{\hat{\boldsymbol{\theta}}_1^T \mathbf{H}^T \mathbf{H} \hat{\boldsymbol{\theta}}_1}{\sigma_w^2} \begin{matrix} > \\ < \end{matrix} \gamma \quad \begin{matrix} \mathcal{H}_1 \\ \mathcal{H}_0 \end{matrix} \tag{10}$$

in which $\hat{\boldsymbol{\theta}}_1 = \left(\mathbf{H}^T\mathbf{H}\right)^{-1}\mathbf{H}^T\mathbf{x}$. The numerator of $T(\mathbf{x})$ can be rewritten as $\mathbf{x}^T\mathbf{H}\left(\mathbf{H}^T\mathbf{H}\right)^{-1}\mathbf{H}^T\mathbf{x}$. The noise variance, σ_w^2, may be incorporated in γ since it is assumed to be constant.

In order for the algorithm to operate in sliding time, a new hypothesis test must be made for each successive sample. In this case a new signal vector, which is overlapping the previous one except for one sample, is used for the new test. Following a detection, a refractory period is introduced, preventing multiple detections from a single event.

D. Algorithm complexity

An important issue when designing pacemaker algorithms is algorithm complexity. The present detector has been designed taking into account complexity constraints by e.g., using small integers in the filters and a recursive structure. Essentially, only two calculations takes place in the detector; the wavelet decomposition resulting in $\mathbf{H}^T\mathbf{x}$ and the test computation $\mathbf{x}^T\mathbf{H}\left(\mathbf{H}^T\mathbf{H}\right)^{-1}\mathbf{H}^T\mathbf{x}$.

It is possible to implement the chosen wavelet structure efficiently by using only shifts and additions. For each sample and scale the lowpass filtering with $f(n)$ requires 4 additions and 1 shift. Similarly, the double use of $g_a(n)$ results in 2 additions. However, due to different gains among the filter bank scales, a rough normalization using shift operations is also necessary in a fixed point implementation.

Calculating $T(\mathbf{x})$ is somewhat more demanding. However, $\left(\mathbf{H}^T\mathbf{H}\right)^{-1}$ is fixed which reduces complexity significantly. Moreover, $\left(\mathbf{H}^T\mathbf{H}\right)^{-1}$ is symmetric and sparse with half of its elements equal to zero due to orthogonality between symmetric and antisymmetric functions. An efficient implementation is obtained by expressing $T(\mathbf{x})$ as,

$$T(\mathbf{x}) = \sum_{i=1}^{p}\sum_{j=1}^{p}\left(\mathbf{H}^T\mathbf{H}\right)^{-1}_{i,j}\mathbf{x}^T\mathbf{H}_i\mathbf{H}_j^T\mathbf{x} \tag{11}$$

and rewriting it by completing the square. By also considering the properties of $\left(\mathbf{H}^T\mathbf{H}\right)^{-1}$, the total number of multiplications can be reduced to $\frac{p^2}{2}+2$ and the number of additions to $\frac{p}{2}\left(\frac{p}{2}+1\right)-1$ for each sample.

In total, using scales 2 – 4 results in 34 additions, 20 multiplications and 7 shifts per sample. Naturally, depending on the implementation, some control operations must be added which are not considered above.

IV. Results

In order to evaluate the presented method, some common noise signals were added to the signals in the EGM database to model noisy environments.

A. Performance measures

Two performance measures were calculated, the *sensitivity*, S, and the *positive predictivity*, P^+,[2]

$$S = \frac{N_T}{N_T + N_M} \qquad P^+ = \frac{N_T}{N_T + N_F} \tag{12}$$

[2]This notation differs from detection theory where the *probability of detection*, P_D and *probability of false alarm*, P_{FA} are used. The relation between the two sets is $P_D = S$ and $P_F = 1 - P^+$, respectively.

where N_T is the number of true detections, N_M is the number of missed detections and N_F is the number of false detections. A total of 3367 annotated events were found in the database.

B. Noiseless performance

Although it is important for an event detector to handle high interference levels, most of the time, the pacemaker is operating in low noise environments. For this reason, a brief part is included considering the noiseless performance. The overall no-noise performance was $S = 0.998$, $P^+ = 1$ with the threshold $\gamma = \eta \check{\boldsymbol{\theta}}_1^T \mathbf{H}^T \mathbf{H} \check{\boldsymbol{\theta}}_1$ where $\check{\boldsymbol{\theta}}_1$ was calculated as the median of $\hat{\boldsymbol{\theta}}_1$ of the ten first R waves in each recording, cf. Table I.

TABLE I
NOISELESS PERFORMANCE.

Threshold, η	$1 - S$, $[\times 10^{-3}]$	$1 - P^+$, $[\times 10^{-3}]$
0.3	2.0	21
0.4	2.3	0
0.5	2.7	0
0.6	4.9	0
0.7	23	0

C. Performance in noise

Performance was evaluated for two noise levels, 20 dB and 25 dB. For each noise level, the results for three levels of η are presented, cf. Fig 3. It is shown in Fig. 3 (a) that S decreases for increasing η for all noise sources at 25 dB SNR. Regarding P^+, it is noted that values close to 1 are obtained for all types of noise and all η. Looking into the higher noise level in Fig. 3 (b), the performance from the different noise types is more widely spread. While performance for both the power drill and the hand mixer mainly decrease in S for increasing η, having a constant P^+, more pronounced changes are found for both S and P^+ in the other categories. In general, the worst performance is found for the Esselte System 2500 and for the muscular noise.

V. Discussion

The scope of this study was to design a low-complexity event detector. The detector is using a linear combination of symmetric and antisymmetric functions of different widths to model the basic EGM waveforms. By using a dyadic wavelet decomposition with short integer filters, the result is a low complexity detector structure. Considering the complexity of the algorithm, a robust functionality is achieved for moderate to high noise levels.

Within this study no word length evaluation have been included. Consequently, all results are based on double precision computations. Still, a proper fixed point word length selection is expected to only marginally alter the results.

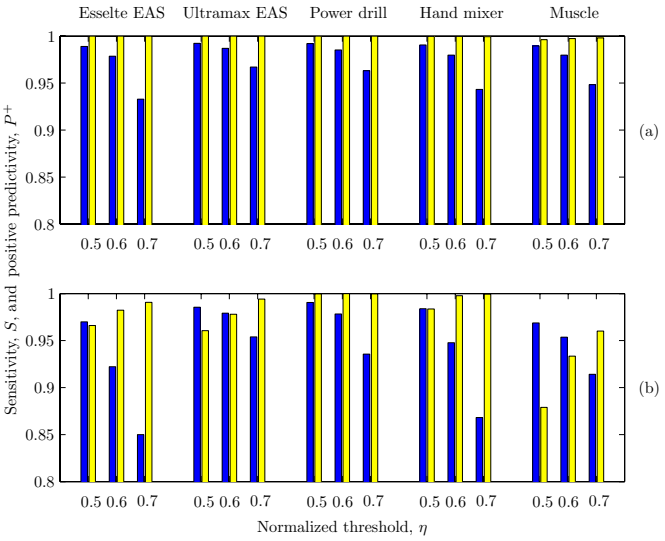

Fig. 3. Performance for different external noise and threshold values in terms of S (darker bars) and P^+ (brighter bars). In (a), the performance for the four noise sources is shown for 25 dB while in (b), the same is shown for 20 dB.

The GLRT detector among other detection principles maximizes P_D for a constant P_{FA}. In order for this to hold, both the signal and the noise must be estimated, cf. (9). However, in this paper the noise level was assumed to be constant. Introducing a noise level estimation in the detector, assuming that it can be done to a low cost, is likely to improve the performance in a noisy environment.

References

[1] R. Sanders and M. Lee, "Implantable pacemakers," *Proc. IEEE*, vol. 84, pp. 480–486, March 1996.

[2] W. Irnich, "Interference in pacemakers," *PACE*, vol. 7, pp. 1021–1048, November-December 1984.

[3] D. Hayes, P. Wang, D. Reynolds, M. Estes, J. Griffith, R. Steffens, G. Carlo, G. Findlay, and C. Johnson, "Interference with cardiac pacemakers by cellular telephones," *The New England Journal of Medicine*, vol. 336, pp. 1473–1479, May 1997.

[4] J. Gimbel, R. Lorig, and B. Wilkoff, "Survey of magnetic resonance imaging in pacemaker patients," *HeartWeb*, vol. 1, October 1996. URL:http://www.heartweb.org/.

[5] E. Lucas, "The effect of electronic article surveillance systems on permanent cardiac pacemakers," *PACE*, vol. 17, pp. 2021–2026, November 1994.

[6] M. McIvor, J. Reddinger, E. Floden, and R. Sheppard, "Study of pacemaker and implantable cardioverter defibrillator triggering by electronic article surveillance devices," *PACE*, vol. 21, pp. 1847–1861, October 1998.

[7] W. Irnich, "Muscle noise and interference behaviour in pacemakers: A comparative study," *PACE*, vol. 10, pp. 125–132, January-February 1987.

[8] W. Irnich, "Intracardiac electrograms and sensing test signals: Electrophysiological, physical and technical considerations," *PACE*, vol. 8, pp. 870–888, November-December 1985.

[9] S. Mallat, *A wavelet tour of signal processing*. San Diego, CA, USA: Academic Press, 1998.

[10] S. Kay, *Fundamentals of statistical signal processing : detection theory*, vol. II. Upper Saddle River, NJ, USA: Prentice Hall, 2 ed., 1998.